

A Robust Resource Allocation Algorithm for Packet BIC-UFMC 5G Wireless Communications

Paolo Del Fiorentino, Carmine Vitiello, Vincenzo Lottici, Filippo Giannetti and Marco Luise
Department of Information Engineering, University of Pisa, I-56122 Pisa, Italy

Abstract—In this paper, we present a novel resource allocation (RA) algorithm for packet Universal Filtered Multi-Carrier (UFMC) BIC-based communications, the latter being a novel modulation format possibly envisaged to be applied in 5G wireless systems. Assuming the perfect knowledge of the channel and capitalizing on the specific UFMC signal waveform, the proposed RA strategy optimizes the coding rate and bit loading within the overall bandwidth along with the per-subband power distribution. In the presence of a carrier offset and over fading selective channels, the results we obtained are twofold: *i*) the UFMC format reveals to be more robust than the conventional OFDM scheme; *ii*) the performance of the UFMC system itself is further boosted by the optimal choice of radio resources evaluated by the proposed RA algorithm.

I. INTRODUCTION

The changes of mobile traffic characteristics lead to fifth-generation (5G) communication techniques evolution. In particular, the most important process of changing is given by the advent of the Internet of Things (IoT), where mobile network would support wireless communications between hundreds of entities with really different requirements, in terms of bit rate, latency and so on. For this reason, efficient use of transmission resources represents the main challenge for researchers involved into the development of the 5G mobile network [1]. Traditional multicarrier modulation developed for fourth-generation (4G) networks, i.e. OFDM, shows advantages on ease modulation and demodulation algorithm and great robustness against fading, achieving efficiency of high-rate mobile communications. But whole features are unfeasible with new requirements of the IoT, as in the case of Machine-Type Communication (MTC), where connections are established between low cost nodes (below 10 \$) with long life time (greater than 10 years) [2]. Indeed, OFDM exploits strictly synchronization procedure to preserve orthogonality, which are in contrast with energy saving principle of the IoT. Therefore, OFDM appears unsuitable for a 5G network, because if the synchronization procedure is not perfect, Inter Carrier Interference (ICI) occurs and the system performance falls down. Furthermore, side-lobe level results too invasive for spectrum sharing, CP length decreases spectral efficiency and latency doesn't allow real-time communication, i.e. for Tactile Internet [2]. For these reasons many new waveform are proposed. FilterBank Multi-Carrier (FBMC) provides per-subcarrier filtering, increasing robustness with misalignment effects, but it also has some drawbacks for certain MIMO schemes and spectral efficiency decreases due to filter length for having narrow filtering. UFMC represents a tradeoff be-

tween OFDM and FBMC [3]. Subcarriers are grouped into subbands, in which IFFT and filtering are performed. In this way, UFMC allows to increase robustness against both time and frequency misalignment, having a good spectral efficiency and without losing OFDM quality.

In this paper, we present a solution to further increase the efficiency of a UFMC transmission w.r.t. the classic OFDM system. In detail, a bit interleaved coded (BIC) modulation [4] and a resource allocation (RA) mechanism are exploited. The derived RA technique selects the optimal modulation format, coding rate and power allocation (PA) vector per subbands in order to maximize a particular performance metric called Goodput (GP) [5]. In particular, the objective function of the RA problem is an estimation of the GP, called (EGP) that has been presented in [6]. Numerical results present the efficiency in terms of GP of the RA for BIC-UFMC, which has been compared with the BIC-OFDM model. Simulations examine the case with perfect synchronization and then with residual Carrier Frequency Offset (CFO).

Notations. Vectors are in bold, $[\cdot]^T$ is the transpose operator, $[x]$ is the lower integer of x and $[x]^+ \triangleq \max\{0, x\}$.

II. SYSTEM MODEL

BIC-UFMC and BIC-OFDM systems operate within a band B_{sys} that is composed of N subcarriers with an available power P_{tot} . Perfect synchronization and perfect knowledge of the channel is assumed. Moreover, the frequency-selective fading channel is considered stationary for the whole transmission duration of a packet and it includes the path loss. Each transmitted packet consists of N_u bits, N_p of which are information and N_{CRC} are cyclic redundancy check (CRC). At the first stage, the packets are processed by the BIC modulation block. The N_u bits are first encoded using an error-correcting code with rate $r \in \mathcal{D}_r \triangleq \{r_0, \dots, r_{|\mathcal{D}_r|}\}$, thus obtaining N_c coded bits that are subsequently randomly interleaved. Then, coded bits are Gray-mapped into N_s complex symbols, which are transmitted in $N_f \triangleq N_s/N$ frames. Uniform bit allocation (UBA) over the subcarriers belonging to the overall band B_{sys} is considered, therefore, the generic frame is $\mathbf{s}^{(v)} \triangleq [s^{(v)}(0), \dots, s^{(v)}(N-1)]^T$, $1 \leq v \leq N_f$, where $s^{(v)}(n)$, $\forall n \in \mathcal{N} \triangleq \{0, \dots, N-1\}$, belongs to the unit-energy constellation $\chi \triangleq 2^{m_v}$ -QAM, being $m_v \in \mathcal{D}_m \triangleq \{2, \dots, m_{\text{max}}\}$ the number of bits allocated per subcarrier. After the BIC stage, the signal can be processed by either UFMC or OFDM transmitter. In order to simplify the notation, index v is dropped in the remainder of this article.

A. BIC-UFMC Signal Model

The classical architecture of the UFMC modulator is depicted in Fig. 1. At the first stage, the frame of QAM symbols \mathbf{s} is split into B subbands, each one composed by $D \triangleq N/B$ subcarriers, obtaining $\mathbf{s}_i \triangleq [s(iD), \dots, s(iD + D - 1)]^T$, where $i \in \mathcal{B} \triangleq \{0, \dots, B - 1\}$ represents subband index. After, \mathbf{s}_i is element-wise multiplied by the square root of $\mathbf{p}_i \triangleq [p(iD), \dots, p(iD + D - 1)]^T$, which is a partition on PA vector $\mathbf{p} \triangleq [p(0), \dots, p(N - 1)]^T$, that must satisfy the following constraint: $\sum_{n=0}^{N-1} p(n) \leq P_{\text{tot}}$. Subsequently, $N_{\text{FFT}} - D$ virtual subcarriers are added to the vector $\sqrt{\mathbf{p}_i} \mathbf{s}_i$ defining zeropadded version named $\sqrt{\mathbf{p}_i^{\text{zp}}} \mathbf{s}_i^{\text{zp}}$ and then an IFFT with size N_{FFT} is performed, obtaining in time-domain the block of samples \mathbf{x}_i , whose generic element is expressed as

$$\begin{aligned} x_i(u) &= \sum_{k=0}^{N_{\text{FFT}}-1} \sqrt{p_i^{\text{zp}}(k)} s_i^{\text{zp}}(k) e^{j\frac{2\pi k u}{N_{\text{FFT}}}} = \\ &= \sum_{k=iD}^{iD+D-1} \sqrt{p(k)} s(k) e^{j\frac{2\pi k u}{N_{\text{FFT}}}}. \end{aligned} \quad (1)$$

where $u = 0, \dots, N_{\text{FFT}} - 1$. Then vector \mathbf{x}_i is convolved with a Dolph-Chebyshev finite impulse response (FIR) filter with 60 dB side lobe attenuation and length L . The generic sample of the impulse response $q(l)$ is shifted in the i -th subband by normalized frequency shift defined as $\Delta_i \triangleq \frac{D+1}{2} + iD$, obtaining $q_i(l) \triangleq q(l) e^{j\frac{2\pi \Delta_i l}{N_{\text{FFT}}}}$, where $l = 0, \dots, L - 1$. The output of each filter, therefore, provides the vector \mathbf{z}_i , whose generic u -th element $z_i(n)$ can be expressed as

$$z_i(u) = \sum_{m=0}^{N_{\text{FFT}}-1} x_i(m) q_i(u - m). \quad (2)$$

where $u = 0, \dots, N_{\text{FFT}} + L - 1$. The vectors of all subbands are then element-wise summed, in order to obtain $\mathbf{z} \triangleq \sum_{i=0}^{B-1} \mathbf{z}_i$, and the resulting vector \mathbf{z} is transmitted over a frequency-selective fading channel, with impulse response \mathbf{h} . For avoiding overlapping between adjacent multicarrier symbols, preserving the orthogonality of the signal, a guard interval is used for transmitting each UFMC symbol. At the receiver side, the signal in the time-domain is described, after the convolution with the channel impulse response, as

$$r(l) \triangleq \sum_{m=0}^{N_{\text{FFT}}+L-1} z(m) h(l - m) + w(l), \quad (3)$$

where $l = 0, \dots, N_{\text{FFT}} + L + L_{\text{CH}} - 3$, L_{CH} is the length of the channel impulse response and $w(l) \in \mathcal{CN}(0, \sigma^2)$ is a complex-valued sample of Gaussian noise. In order to avoid self-interference contribution over the useful subcarriers, an FFT with order $2N_{\text{FFT}}$ is performed on the whole received signal, composed by $N_{\text{FFT}} + L + L_{\text{CH}} - 2$ samples, followed by a downsampling by a factor 2 and taking only the even-indexed subcarriers as suggested in [7]. By this way, the k -th subcarrier in the frequency domain results

$$Y(k) = H(k) \sum_{i=0}^{B-1} Q_i(k) X_i(k) + W(k), \quad (4)$$

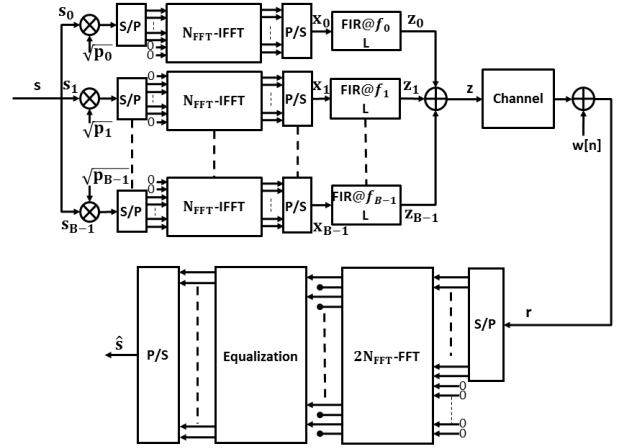


Fig. 1. Architecture of UFMC transceiver

where $k = 0, 2, \dots, 2N_{\text{FFT}} - 2$, $H(k)$, $Q_i(k)$, $X_i(k)$ and $W(k)$ represent the generic k -th element of the $2N_{\text{FFT}}$ -FFT output relevant to channel impulse response \mathbf{h} , filter impulse response \mathbf{q}_i , symbols \mathbf{x}_i and ambient noise, respectively. Finally, the signal (4) is equalized by a zero forcing (ZF) equalizer and soft-decoded. Under the hypothesis of perfect synchronization and bearing in mind (1), $X_i(k)$ can be written, $\forall i \in \mathcal{B}$, as

$$X_i(k) \triangleq \begin{cases} \sqrt{p(\frac{k}{2})} s(\frac{k}{2}), & \text{for } \frac{k}{2} = iD, \dots, iD + D - 1 \\ 0, & \text{otherwise} \end{cases}. \quad (5)$$

In this case eq. (4) becomes

$$Y(n) \triangleq H(n) Q_{i(n)}(n) \sqrt{p(n)} s(n) + W(n), \quad (6)$$

with $n \in \mathcal{N}$ and $i(n) \triangleq \lfloor n/D \rfloor$, $i(n) \in \mathcal{B}$. Finally, the received SNR for unit power transmission is equal to

$$\gamma_{\text{ufmc}}(n) \triangleq \frac{|H(n)|^2 |Q_{i(n)}(n)|^2}{\sigma^2}, \quad (7)$$

and the received SNR vector is defined as $\boldsymbol{\Gamma}_{\text{ufmc}} \triangleq [p(0)\gamma_{\text{ufmc}}(0), \dots, p(N-1)\gamma_{\text{ufmc}}(N-1)]^T$.

B. BIC-OFDM Signal Model

The BIC-OFDM model is recalled from [6]. The vector \mathbf{s} is element-wise multiplied by the square root of the PA vector \mathbf{p} , it passes through N_{FFT} -IFFT and after cyclic prefix (CP) insertion. At the receiver, N_{FFT} -FFT is performed, after a frequency equalization and finally the signal is soft-decoded. The received sample $Y(n)$ over the subcarrier n in the frequency-domain is

$$Y(n) \triangleq \sqrt{p(n)} H(n) s(n) + W(n), \quad (8)$$

where $H(n)$ is the frequency channel coefficient and $W(n)$ is the ambient noise. The received SNR for unit power transmission over the subcarrier n is

$$\gamma_{\text{ofdm}}(n) \triangleq \frac{|H(n)|^2}{\sigma^2}, \quad (9)$$

and the received signal to noise ratio (SNR) vector is defined as $\mathbf{\Gamma}_{\text{ofdm}} \triangleq [p(0)\gamma_{\text{ofdm}}(0), \dots, p(N-1)\gamma_{\text{ofdm}}(N-1)]^T$.

III. GOODPUT METRIC

In this section we consider a generic multicarrier system with N subcarriers, hence the description that follows is valid for both BIC-UFMC and BIC-OFDM models. As discussed in Sect. II, practical modulation and coding schemes are employed, therefore, the GP, which is defined as the number of correctly received information bits per unit of time [8] is a very metric for providing a reliable picture of the link performance. In order to get an estimate of the GP, i.e. the EGP, the κ effective SNR mapping (κ ESM) link performance prediction (LPP) method is exploited, because it combines together the simplicity of the exponential ESM (EESM) with the accuracy of the mutual information ESM (MIESM) as shown in [6]. In detail, the EGP function depends on the packet error rate (PER) of the link, but unfortunately, the closed-form expression of the PER for coded multicarrier systems over frequency-selective channels is hard to derive. The solution for this problem is given by the κ ESM technique [6], which compresses the vector of the received SNRs $\mathbf{\Gamma} \triangleq [p(0)\gamma(0), \dots, p(N-1)\gamma(N-1)]^T$ into a single SNR value γ_{eff} , called *effective* SNR. Given a transmission mode $\phi \triangleq (r, m) \in \mathcal{D}_r \times \mathcal{D}_m$ and a PA vector \mathbf{p} , such a SNR value γ_{eff} is used to estimate the PER from an equivalent coded BPSK system over an AWGN channel, so that

$$\text{PER}_{\phi}(\mathbf{\Gamma}) \cong \Phi_r(\gamma_{\text{eff}}), \quad (10)$$

where PER_{ϕ} and Φ_r denote the PER of the coded multicarrier system over frequency-selective channel for a TM ϕ and that of the equivalent coded BPSK system over AWGN channel experiencing the *effective* SNR, respectively. The κ ESM expression is defined as [6]

$$\gamma_{\text{eff}} \triangleq -\log \left[\frac{1}{Nm} \cdot \sum_{n=1}^N \alpha_n \cdot e^{-p(n)\gamma(n)\beta_n} \right], \quad (11)$$

with α_n and β_n constant values depending on the size m of the modulation constellation.

Exploiting κ ESM method for LPP, the EGP function can be expressed in bit/s/Hz as

$$\begin{aligned} \zeta(\phi, \mathbf{p}) &\triangleq \frac{N_{\text{FFT}}}{N_{\text{FFT}} + L + L_{\text{CH}} - 2N} \frac{T_s N_p [1 - \Phi_r(\gamma_{\text{eff}})]}{\frac{N_u T_s}{rNm}} = \\ &= \frac{N_{\text{FFT}}}{N_{\text{FFT}} + L + L_{\text{CH}} - 2N_u} \frac{N_p}{N_u} r m [1 - \Phi_r(\gamma_{\text{eff}})], \end{aligned} \quad (12)$$

where $B_{\text{sys}} \triangleq N/T_s$ is the occupied RF bandwidth, T_s is the sample time and $N_u T_s / rNm$ is the packet transmission time.

IV. EGP-BASED RA FOR BIC-UFMC SYSTEMS

The RA method for BIC-UFMC systems is based on the maximization of the EGP function (12) under the assumption of perfect knowledge of the channel state information (CSI), which is represented by the vector of the received SNRs for

unit power transmission. In detail, the key idea behind the EGP-based RA is to calculate $\mathbf{p}_i^* \triangleq [p^*(iD), \dots, p^*(iD + D - 1)]^T$ that minimizes the PER (10) of each subband. Subsequently, the optimal TM $\phi^* \triangleq (r^*, m^*)$ is evaluated by maximizing the overall EGP (12) of the system. This approach is feasible since the subcarriers belonging to a subband are always orthogonal to each other. Here perfect synchronization is assumed, thus orthogonality is preserved among all N subcarriers of the system as explained in Sec. II-A. In light of the above, the RA problem is divided in two steps.

A. PA Solution

The PA vector \mathbf{p}_i^* is derived, given a generic TM ϕ , by solving the following optimization problem (OP)

$$\begin{aligned} \mathbf{p}_i^* &= \arg \min_{\mathbf{p}_i} \left\{ \Phi_r^{(i)}(\gamma_{\text{eff}}^{(i)}) \right\} \\ \text{s.t.} \quad &\sum_{d=0}^{D-1} p(iD + d) \leq P_B, \quad \forall i \in \mathcal{B}, \end{aligned} \quad (13)$$

where $\Phi_r^{(i)}$ is the PER for the subband i , $P_B \triangleq P_{\text{tot}}/B$, i.e. uniform subband power allocation is considered, and $\gamma_{\text{eff}}^{(i)}$ is

$$\gamma_{\text{eff}}^{(i)} \triangleq -\log \left[\frac{1}{Nm} \cdot \sum_{d=0}^{D-1} \alpha_d^{(i)} \cdot e^{-p(iD+d)\gamma_{\text{ufmc}}(iD+d)\beta_d^{(i)}} \right]. \quad (14)$$

The OP (13) is solved by maximizing the argument of the PER $\Phi_r^{(i)}$ and consequently by minimizing the numerator of the log function (14). Thus, the PA problem changes in

$$\begin{aligned} \mathbf{p}_i^* &= \arg \min_{\mathbf{p}_i} \{ \psi(\mathbf{p}_i) \} \\ \text{s.t.} \quad &\sum_{d=0}^{D-1} p(iD + d) \leq P_B, \\ &p(iD + d) \geq 0, \quad d = 0, \dots, D - 1 \end{aligned} \quad (15)$$

where the new objective function is

$$\psi(\mathbf{p}_i) \triangleq \sum_{d=0}^{D-1} \alpha_d^{(i)} e^{-p(iD+d)\gamma_{\text{ufmc}}(iD+d)\beta_d^{(i)}}. \quad (16)$$

The PA problem (15) is convex [9], and therefore its solution is calculated with the method of Lagrange multipliers.

Starting from (15), the Lagrangian can be written

$$\begin{aligned} \mathcal{L}(p(iD)^*, \dots, p^*(iD + D - 1), \lambda_0, \dots, \lambda_{D-1}, \theta) &\triangleq \\ &\triangleq \sum_{d=0}^{D-1} \alpha_d^{(i)} e^{-p^*(iD+d)\gamma_{\text{ufmc}}(iD+d)\beta_d^{(i)}} - \\ &- \sum_{iD=0}^{D-1} \lambda_d p^*(iD + d) + \theta \left(\sum_{d=0}^{D-1} p^*(iD + d) - P_B \right), \end{aligned} \quad (17)$$

where $\lambda_0, \dots, \lambda_{D-1}, \theta$ are the Lagrange multipliers. By applying the Karush-Kuhn-Tucker (KKT) conditions [9], the following expression is obtained

$$\begin{aligned} \frac{\partial \mathcal{L}}{\partial p^*(iD + d)} &\triangleq -\alpha_d^{(i)} \gamma_{\text{ufmc}}(iD + d) \beta_d^{(i)} \cdot \\ &\cdot e^{-p^*(iD+d)\gamma_{\text{ufmc}}(iD+d)\beta_d^{(i)}} - \lambda_d + \theta = 0, \end{aligned} \quad (18)$$

Initialize: $m = 0, \zeta_{\max} = 0;$
Start: Set $m = m + 2;$
For $i = 0 : B - 1$
 Evaluate $\bar{\mathbf{p}}_i(m);$
End For
Collect $\bar{\mathbf{p}}(m) = [\bar{\mathbf{p}}_0(m), \dots, \bar{\mathbf{p}}_{B-1}(m)]^T;$
Select $r' = \arg \max_{r \in \mathcal{D}_r} \{\zeta(r, m, \bar{\mathbf{p}}(m))\};$
If $\zeta(r', m, \bar{\mathbf{p}}(m)) \geq \zeta_{\max}$
 Set $m^* = m, r^* = r', \mathbf{p}^* = \bar{\mathbf{p}}(m), \zeta_{\max} = \zeta(r', m, \bar{\mathbf{p}}(m));$
End If
If $m \neq m_{\max}$
 Go to Start;
Else
 Return $\phi^* = \{m^*, r^*\}$ and $\mathbf{p}^*;$
End If

TABLE I
EGP-BASED RA

$$p^*(iD + d) \geq 0, \quad (19)$$

$$\sum_{d=0}^{D-1} p^*(iD + d) \leq P_B, \quad (20)$$

$$\lambda_d \geq 0, \quad (21)$$

$$\lambda_d \cdot p^*(iD + d) = 0. \quad (22)$$

Thus from (18), λ_d is obtained, which is replaced in (22). According to (19) (21), the optimal power $p^*(iD + d)$, for $d = 0, \dots, D - 1$, is found as

$$p^*(iD + d) \triangleq \frac{1}{\gamma_{\text{ufmc}}(iD + d) \beta_d^{(i)}} \left[\log \frac{1}{\theta} - \log \left(\frac{1}{\gamma_{\text{ufmc}}(iD + d) \alpha_d^{(i)} \beta_d^{(i)}} \right) \right]^+ \quad (23)$$

The solution (23) is a typical water-filling solution [9]. The PA solutions are collected as $\mathbf{p}^* \triangleq [\mathbf{p}_0^*, \dots, \mathbf{p}_{B-1}^*]^T$.

B. TM Solution

The Optimal TM $\phi^* \triangleq (r^*, m^*)$ is evaluated by maximizing the overall EGP (12) as follows

$$\begin{aligned} \phi^* &= \arg \max_{\phi} \{\zeta(\phi, \mathbf{p}^*)\} \\ \text{s.t. } &\phi \in \mathcal{D}_r \times \mathcal{D}_m \end{aligned}, \quad (24)$$

which is exhaustively solved. Table I shows a pseudo-code of the EGP-based RA.

Proposition. Optimal TM ϕ^* and PA vector \mathbf{p}^* for a BIC-OFDM system are evaluated as a special case of the EGP-based RA for BIC-UFMC of Sec. IV, considering a subband, i.e. $B = 1$. ■

The effectiveness of the proposed RA technique for a packet BIC-UFMC modulation is provided on the basis of a comparison in terms of GP with a classic BIC-OFDM model. The set of simulation parameters is summarized in Tab. II. Moreover, extended vehicular A (EVA) channel [10] and modified COST231 Hata path loss (PL) [11] models are used. Dolph-Chebyshev FIR filter length is $L = 73$. In order to ensure a correct comparison between BIC-UFMC and BIC-OFDM, cyclic prefix is set to $\nu \triangleq L - 1$ [12]. In this way transmitted signal of both waveforms has same length. Convolutional code is exploited to simplify the processing of the soft-decoded, however, turbo code can be considered, by adding an adjusting factor in eq. (14) as in [13]. GP performance is evaluated by averaging the number of bits/s/Hz correctly received on $N_{\text{pkt}} = 1000$ transmitted packet for each SNR. Thus, the average GP (AGP) is defined as $\text{AGP} \triangleq \frac{N_{\text{FFT}}}{N_{\text{FFT}} + L + L_{\text{CH}} - 2} \frac{1}{N_{\text{pkt}}} \frac{1}{B_{\text{sys}}} \sum_{s=1}^{N_{\text{pkt}}} \frac{N_p \delta(s)}{T_{\text{pkt}}(s)}$, where $\delta(s)$ equals 1 if the s -th packet is correctly decoded and 0 when it is discarded, $T_{\text{pkt}}(s)$ is the transmission time of the s -th packet. Finally, each transmitted packet experiences independent channel realizations and the SNR points are calculated as $\text{SNR} \triangleq P_{\text{tot}} / (P_{\text{noise}} \Theta)$ by varying P_{tot} , with Θ the PL value. Firstly, Fig. 2 verifies the effectiveness of the EGP-based RA by comparing EGP and AGP values. As can be seen, the resulting value of AGP is equal to the EGP $\zeta(\phi^*, \mathbf{p}^*)$. Therefore, the RA technique is able to correctly choose the optimal transmission parameters in terms of \mathbf{p}^* and ϕ^* . Introducing a frequency misalignment, such as CFO as shown in [7] and applying EGP-based RA, we are able to highlight BIC-UFMC features in terms of robustness of coarse synchronization. The expression of the CFO in the time-domain for the i -th subband can be explicit as $c_i(k) \triangleq e^{\frac{j2\pi e_i k}{N_{\text{fft}}}}$, where $k = 0, \dots, N_{\text{fft}} + L - 1$ and e_i represents the CFO normalized to the subcarrier spacing. The same CFO for each BIC-UFMC subband is considered in order to ensure a fair comparison with the BIC-OFDM system, which has the same CFO for whole band. So we intentionally break the orthogonality among the subcarriers, introducing Inter-Band Interference (IBI) and Inter-Carrier Interference (ICI). First of all, it is possible to appreciate improvements due to the RA strategy on BIC-UFMC. As we show in Fig. 3 at SNR= 10dB, optimal PA (OPA) on BIC-UFMC improves AGP when CFO is included in $[\pm 0.03]$, w.r.t. uniform PA (UPA) (optimal TM is always considered). Since the RA has been designed without caring of the presence of a possible CFO, outside the above interval, the AGP performance with RA degrades similarly as that without RA. As expected we can theoretically think and as depicted in Fig. 4 at SNR= 36dB, where the noise can be neglected, the filtering attenuates interference effect: for CFO values around 0, AGP results equivalent in both BIC-UFMC and BIC-OFDM system but increasing misalignments, BIC-UFMC shows a slight performance enhancement than BIC-OFDM along whole CFO variation range.

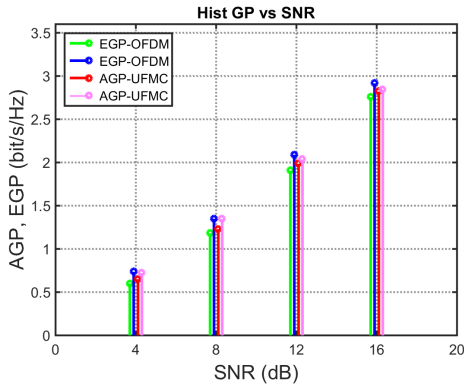


Fig. 2. EGP vs. AGP

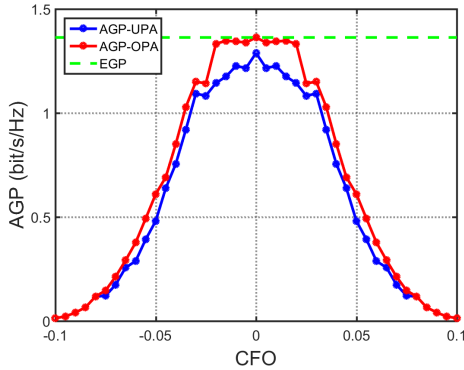


Fig. 3. Optimal PA vs. uniform PA in BIC-UFMC (SNR= 10 dB)

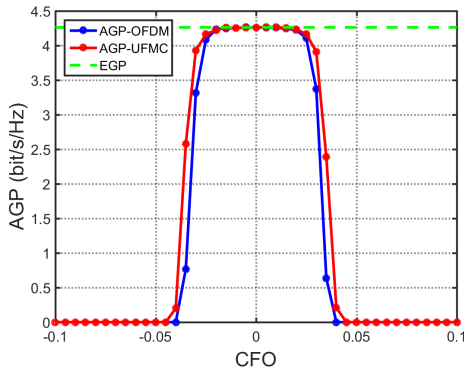


Fig. 4. EGP-based RA for BIC-UFMC and BIC-OFDM (SNR= 36 dB)

VI. CONCLUSIONS

In this paper, we have presented an EGP-based RA strategy intended for BIC-UFMC waveforms. We have shown how to optimally select the coding rate, modulation format and power distribution across subcarriers within each subbands in order to maximize the GP metric. In case of perfect synchronization, BIC-UFMC achieves similar performance as that offered by conventional OFDM. In presence of a CFO, we have demonstrated that: *i*) a slight gain of the former is allowed with respect to the conventional one; *ii*) the RA can further

| Simulation Parameters | Value |
|--|----------------------|
| Information bits (N_p) | 1024 |
| CRC (N_{CRC}) | 32 |
| Subcarriers (N) | 120 |
| Subbands (B) | 10 |
| FFT size | 1024 |
| Bandwidth (B_{sys}) | 10 MHz |
| QAM modulation order (m) | 2, 4, 6 |
| Convolutional code-rate (r) | 1/2, 2/3, 3/4, 5/6 |
| Noise power in B_{sys} (P_{noise}) | -110 dBm |
| Variance ambient noise (σ^2) | P_{noise}/N |
| Distance transmitter-receiver (d) | 141 m |

TABLE II
SYSTEM PARAMETERS

boost performance of BIC-UFMC with respect of uniform PA.

ACKNOWLEDGMENT

This work has been partially supported by the PRA 2016 research project 5GIOTTO funded by the University of Pisa.

REFERENCES

- [1] Andrews, J.G.; Buzzi, S. et al, "What Will 5G Be?", in *Selected Areas in Communications, IEEE Journal on* , vol.32, no.6, pp.1065-1082, June 2014.
- [2] Wunder, G.; Jung, P. et al, "5GNOW: non-orthogonal, asynchronous waveforms for future mobile applications", in *Communications Magazine, IEEE* , vol.52, no.2, pp.97-105, February 2014.
- [3] Schaich, F.; Wild, T., "Waveform contenders for 5G OFDM vs. FBMC vs. UFMC", in *Communications, Control and Signal Processing (ISCCSP), 2014 6th International Symposium on* , vol., no., pp.457-460, 21-23 May 2014.
- [4] Caire, G.; Taricco, Giorgio; Biglieri, Ezio, "Bit-interleaved coded modulation," in *Information Theory, IEEE Transactions on* , vol.44, no.3, pp.927-946, May 1998.
- [5] B. Devillers, J. Louveaux, and L. Vandendorpe, "Bit and power allocation for goodput optimization in coded parallel subchannels with ARQ", *IEEE Trans. on Signal Process.*, vol. 56, no. 8, pp.3652-3661, Aug. 2008.
- [6] Stupia, I.; Lottici, V.; Giannetti, F.; Vandendorpe, L., "Link Resource Adaptation for Multiantenna Bit-Interleaved Coded Multicarrier Systems", in *Signal Processing, IEEE Transactions on* , vol.60, no.7, pp.3644-3656, July 2012.
- [7] Wang, Xiaojie; Wild, Thorsten; Schaich, Frank; Fonseca dos Santos, Andre, "Universal Filtered Multi-Carrier with Leakage-Based Filter Optimization", in *European Wireless 2014; 20th European Wireless Conference, Proceedings of* , vol., no., pp.1-5, 14-16 May 2014.
- [8] D. Qiao, S. Choi and K.G. Shin, "Goodput analysis and link adaptation for IEEE 802.11a wireless LANs", *Mobile Computing, IEEE Transactions on* , vol.1, no.4, pp.278,292, Oct-Dec 2002.
- [9] S. Boyd and L. Vandenberghe, "Convex optimization", *Cambridge Univ. Press*, 2004.
- [10] Extended vehicular A (EVA) channel. Available: <http://www.raymaps.com/index.php/lte-multipath-channel-models/>.
- [11] IEEE 802.16m Evaluation Methodology Document (EMD), "IEEE 802.16m-08/004r2", pp. 143, July 2008.
- [12] Vakilian, V.; Wild, T.; Schaich, F.; ten Brink, S.; Frigon, J.-F., "Universal-filtered multi-carrier technique for wireless systems beyond LTE," in *Globecom Workshops (GC Wkshps), 2013 IEEE* , vol., no., pp.223-228, 9-13 Dec. 2013.
- [13] Stupia, I.; Giannetti, F.; Lottici, V.; Andreotti, R.; Vandendorpe, L.; D'Andrea, A.N., "A greedy algorithm for goodput-oriented AMC in turbo-coded OFDM," in *Future Network and Mobile Summit, 2010* , vol., no., pp.1-8, 16-18 June 2010.